

Numerical Model of Solidification Including Formation of Multiple Shrinkage Cavities

T. Skrzypczak *, L. Sowa, E. Węgrzyn-Skrzypczak

Institute of Mechanics and Machine Design Fundamentals, Częstochowa University of Technology
 Dąbrowskiego 73, 42-200 Częstochowa, Poland

* Corresponding author. E-mail address: t.skrzypczak@imipkm.pcz.pl

Received 18.06.2019; accepted in revised form 23.09.2019

Abstract

Presented paper shows the mathematical and numerical approaches for modelling of binary alloy solidification solved by the Finite Element Method (FEM). The phenomenon of shrinkage cavities formation process is included in the numerical model. Multiple macroscopic cavities can be modelled within the single casting volume. Solid, liquid and gaseous phases with different material properties are taken into account during solidification process. Mathematical model uses the differential equation of heat diffusion. Modification of specific heat is used to describe the heat releasing during liquid-solid phase change. Numerical procedure of shrinkage cavities evolution is based on the recognition of non-connected liquid volumes and local shrinkage computation in the each of them. The recognition is done by the selection of sets of interconnected nodes containing liquid phase in the finite element mesh. Original computer program was developed to perform calculation process. Obtained results of temperature and shrinkage cavities distributions are presented and discussed in details.

Keywords: Solidification process, Castings defects, Shrinkage cavity, Numerical simulation, Finite element method

1. Introduction

Contraction of the liquid, solid as well as the volume loss in the liquid-solid phase change during solidification process of metal alloys is the main reason of the formation process of micro- and macroscopic defects. Macroscopic defects can be of different types, most common are conical pipe shrinkages forming in the upper part of the riser and closed macropores located deeper in the casting [1, 2]. These defects are commonly called "shrinkage cavities". Presented paper focuses on the numerical modelling of the formation process of macroscopic defects. Such defects can be scattered within the casting thus finally one can observe multiple shrinkage cavities.

The volume of the alloy decreases in three stages of casting process. First stage begins at the moment of pouring the mould with liquid material and lasts until the appearance of solid phase. The contraction of liquid material is caused by linear decreasing

of the volume as temperature drops and is one of the reasons of the formation process of pipe shrinkages.

Although mentioned stage influences the process of the pipe shrinkage formation presented work only focuses on the second stage of solidification. It begins at the liquidus temperature and lasts until the entire liquid material is transformed into solid. Volume loss in this stage is mainly caused by the liquid-solid transformation. The same amounts of liquid and solid usually have different densities. Liquid is less dense than solid and occupies greater volume. The difference between volumes of liquid and solid is the main reason of macroscopic defects in the casting. Depending on the shape of the casting and cooling conditions the macroscopic pores filled with gaseous phase can be numerous in the body of the final product.

After the solidification the cooling process in the solid state begins. The contraction of material is caused by the temperature drop and also by the phase transformations of the solid material. It

lasts till the shakeout operation and is neglected in presented paper.

Shrinkage cavity formation process and its numerical modelling is the problem widely investigated in the literature [1-8]. Presented model makes possible the prediction and evolution of multiple disconnected macroscopic cavities within single casting.

2. Mathematical model

Figure 1 shows two dimensional section of the casting with different types of regions. Ω_S is the area occupied by the solid fraction while Ω_{L1} and Ω_{L2} are regions filled with liquid metal. Between solid and liquid regions mushy zone Ω_M is located. It contains mixture of solid and liquid phases. Gaseous phase fills volumetric voids Ω_{G1} and Ω_{G2} which are usually connected to the upper part of liquid regions. Such locations are preferred due to the effect of gravitation. Top level of liquid slowly goes down due to contraction of material during liquid-solid phase transformation and then expanding void is filled with air or another gaseous medium.

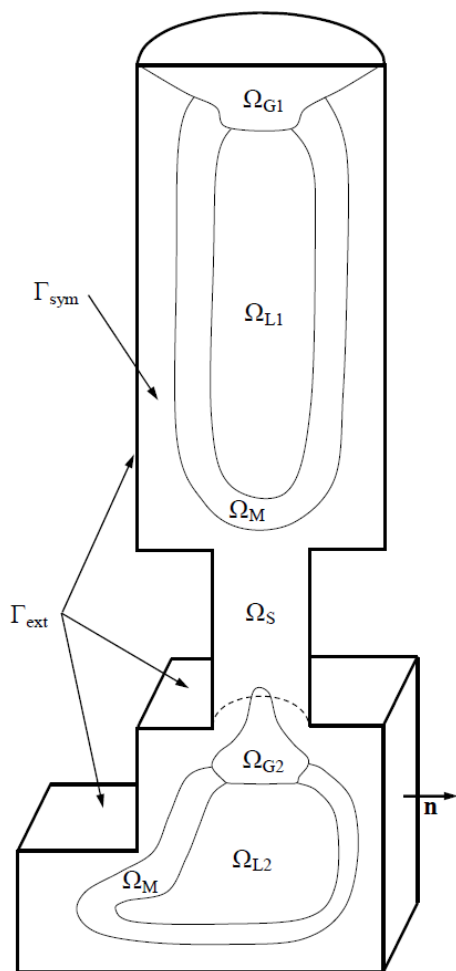


Fig. 1. Scheme of solidifying casting

The base of mathematical description of the problem is the partial differential equation of transient heat transfer (1) together with the appropriate boundary and initial conditions (2-4):

$$\nabla \cdot (\lambda \nabla T) = c \rho \frac{\partial T}{\partial t} \quad (1)$$

Because only half of the casting is considered thermal insulation is applied at the plane of symmetry Γ_{sym} :

$$(x, y, z) \in \Gamma_{sym} : -\mathbf{n} \cdot \lambda \nabla T = 0 \quad (2)$$

Because the geometry of the mould is not explicitly defined in the model the rest of external surfaces of the casting are cooled with the use of Newton boundary condition:

$$(x, y, z) \in \Gamma_{ext} : -\mathbf{n} \cdot \lambda \nabla T = \alpha (T - T_\infty) \quad (3)$$

Initially the entire casting is filled with the molten metal of constant temperature T_0 :

$$T(x, y, z, t = 0) = T_0 \quad (4)$$

where T [K] represents temperature, λ [$\text{J s}^{-1} \text{m}^{-1} \text{K}^{-1}$] describes thermal conductivity, ρ [kg m^{-3}] represents density, c [$\text{J kg}^{-1} \text{K}^{-1}$] is the parameter of effective specific heat which is also used for the proper description of heat releasing during solidification, t [s] represents time, \mathbf{n} denotes vector normal to the external boundary Γ_{ext} , α [$\text{J s}^{-1} \text{m}^{-2} \text{K}^{-1}$] is the heat transfer coefficient, T_∞ [K] is the temperature of external medium (mould or air), T_0 [K] describes initial temperature distribution.

Effective specific heat takes the following form [9]:

$$\begin{aligned} (x, y, z) \in \Omega_S, T < T_S : & \quad c = c_S \\ (x, y, z) \in \Omega_M, T_S \leq T \leq T_L : & \quad c = \frac{c_L + c_S}{2} + \frac{L}{T_L - T_S} \\ (x, y, z) \in \Omega_{L1} \cup \Omega_{L2}, T > T_L : & \quad c = c_L \\ (x, y, z) \in \Omega_{G1} \cup \Omega_{G2} : & \quad c = c_G \end{aligned} \quad (5)$$

where T_L [K] represents liquidus temperature, T_S [K] is solidus temperature, c_L , c_S , c_G [$\text{J kg}^{-1} \text{K}^{-1}$] are the coefficients of specific heat of the liquid, solid and gaseous fractions, L [J kg^{-1}] is the value of latent heat of solidification.

Thermal conductivity λ and density ρ in the liquid, solid, mushy and gaseous regions are calculated in the following way:

$$\begin{aligned} (x, y, z) \in \Omega_{L1} \cup \Omega_{L2} \cup \Omega_{S1} \cup \Omega_{S2} \cup \Omega_M : \\ \lambda = f_L \lambda_L + f_S \lambda_S, \quad \rho = f_L \rho_L + f_S \rho_S \\ (x, y, z) \in \Omega_{G1} \cup \Omega_{G2} : \\ \lambda = \lambda_G, \quad \rho = \rho_G \end{aligned} \quad (6)$$

where λ_L , λ_S , λ_G [$\text{J s}^{-1} \text{m}^{-1} \text{K}^{-1}$], ρ_L , ρ_S , ρ_G [kg m^{-3}] are the coefficients of thermal conductivity and density of the liquid, solid and gaseous phases respectively while f_L and f_S [-] are

dimensionless, temperature dependent parameters describing the amount of liquid and solid fractions:

$$f_S = \frac{T_L - T}{T_L - T_S}, \quad f_L = 1 - f_S \quad (7)$$

Equation (5) shows significant increase of effective specific heat in the mushy zone due to releasing of heat during solidification. In the shrinkage cavities the properties of air are introduced. Presented model permits liquid, solid, liquid-solid and gaseous regions and forbids mixture of gas with another phases. Material properties c , ρ , λ are constant in the liquid, solid and gaseous regions. In the mushy zone they are linear functions of temperature. Heat transfer coefficient α and ambient temperature T_∞ don't change according to time.

3. Numerical model

FEM formulation of numerical model uses Equation (1) together with boundary-initial conditions (2-4) and starts with the criterion of weighted residuals:

$$\int_{\Omega} w \left[\nabla \cdot (\lambda \nabla T) - c\rho \frac{\partial T}{\partial t} \right] d\Omega = 0 \quad (8)$$

where w is the test function of spatial coordinates and Ω represents total volume of the casting.

Standard Galerkin formulation is used to derive set of spatially discretized equations. For the single finite element (e) the following equation is obtained:

$$\lambda^{(e)} \iint_{\Omega^{(e)}} (\mathbf{D}_x^T \mathbf{D}_x + \mathbf{D}_y^T \mathbf{D}_y + \mathbf{D}_z^T \mathbf{D}_z) d\Omega \mathbf{T} + (c\rho)^{(e)} \iint_{\Omega^{(e)}} \mathbf{N}^T \mathbf{N} d\Omega \dot{\mathbf{T}} = - \int_{\Gamma^{(e)}} \mathbf{N} q d\Gamma \quad (9)$$

where \mathbf{N} contains shape functions of finite element, \mathbf{D}_x , \mathbf{D}_y , \mathbf{D}_z are spatial derivatives of shape functions with respect to x , y , z respectively, \mathbf{T} , $\dot{\mathbf{T}}$ contain nodal values of temperature and its time derivatives, q represents the boundary heat flux.

Finally backward Euler method is used to perform the operation of time discretization and the following scheme is obtained to calculate temperature distribution:

$$\left(\mathbf{K} + \frac{1}{\Delta t} \mathbf{M} \right) \mathbf{T}^{j+1} = \frac{1}{\Delta t} \mathbf{M} \mathbf{T}^j + \mathbf{B} \quad (10)$$

where \mathbf{K} , \mathbf{M} are global matrices of conductivity and heat capacity respectively, \mathbf{B} is the vector containing boundary conditions, Δt [s] denotes time step, j represents current time level.

Important part of presented model is the procedure of multiple shrinkage cavities development process. Similar procedure suitable for single defects was used in [10]. Main assumptions of developed algorithm are as follows:

- The total volume of the casting is divided into nodes.
- Considered casting is initially filled with liquid alloy so each node in the mesh is in the liquid state (L).
- Shrinkage cavities doesn't appear until the start of solidification.
- Algorithm identifies disconnected sets of liquid sub-volumes.
- The solidifying nodes are consequently removed from liquid sub-volumes in the each time step and their summed volume is used to calculate the local shrinkage.
- The local shrinkage is used to change the state of uppermost liquid nodes from (L - liquid) to (G - gaseous). The total volume of such nodes in the each time step equals the volume of calculated local shrinkage.

More detailed description of the used algorithm is presented below.

Before the main calculation loop nodal volumes are computed. Sum of the nodal values equals the volume of the casting:

$$V = \sum_{i=1}^{nm} V_i \quad (11)$$

where nm denotes total number of nodes.

Each time step contains following operations:

- Using known distribution of temperature \mathbf{T}^j and boundary conditions new temperature field \mathbf{T}^{j+1} is obtained according to the scheme (10).
- Nodes with temperature greater than liquidus temperature T_L are marked as liquid. During the pre-solidification stage all nodes are in this state.
- Temperature of the nearest neighbours of liquid node n_i are checked. They are located in the finite elements around n_i (Figure 2). Node can be in the one of four states - liquid (L) mixed (L+S), solid (S) or gaseous (G). If there are neighbours of node n_i marked as liquid (e.g. nodes n_1 and n_2 in Figure 2) they are added to the local set L_k containing all connected liquid nodes.

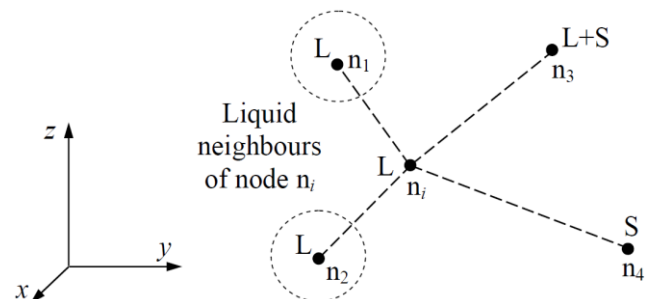


Fig. 2. Nearest neighbours of node n_i

- Neighbourhood of all L-nodes in the mesh are checked. Depending on the shape of the casting and cooling conditions single liquid region ($k=1$) or more separated liquid areas ($k>1$) can be distinguished within the global volume (Figure 3).

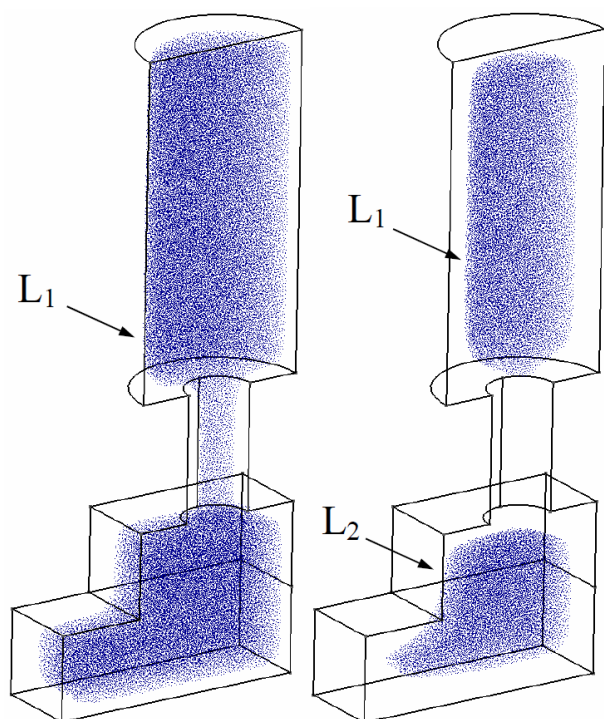


Fig. 3. Identified liquid sub-domains in solidifying casting

- Volume of each identified liquid region is calculated:

$$V_k = \sum_{i=1}^{nnk} V_i \quad (12)$$

where nnk denotes number of nodes in L_k .

- Local shrinkage of solidified material associated with L_k in the current time step is calculated as follows:

$$\Delta S_k = (V_k - \tilde{V}_k) S_h \quad (13)$$

where \tilde{V}_k is the volume of k -th liquid region in the previous time step, S_h represents shrinkage coefficient of liquid-solid phase change.

- Calculated shrink ΔS_k represents the volume increase of the shrinkage cavity associated with k -th region. State of the uppermost nodes in L_k is changed from L (liquid) to G (gaseous). The sum of volumes of G-nodes appearing in the current time step must not be greater than calculated shrink. Remained shrink that cannot be distributed because is smaller than volume of any L-node is memorized for the next step.
- Material properties are actualized because of changes of L-, S- and G-phase distributions. Finally calculations can be done for the next step.

Above operations are repeated until the end of solidification process (Figure 4). Temporary distributions of temperature and shrinkage cavities are saved in the files for later visualisation.

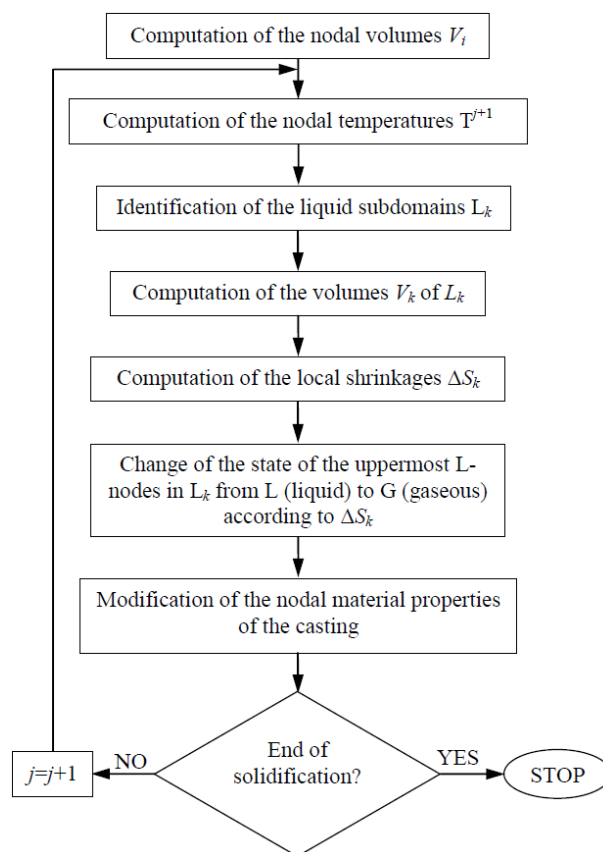


Fig. 4. Algorithm of shrinkage cavities formation process

4. Example of calculations

Geometrical model of the casting with dimensions 375x150x50 mm is prepared using GMSH [11]. GMSH is a non-commercial software designed to provide among others an efficient and fast 3D mesh generator. GMSH contains four modules: mesh, geometry, post-processing and solver but in this work only preparation of geometry and meshing were used. Prepared geometry is meshed with the use of 755112 tetrahedral, 4-node finite elements. Total number of nodes is 146885. It is assumed that the casting is composed of steel containing 0.55% of carbon, which material properties are stored in Table 1.

Table 1.
Material properties used in the model

Material properties	Liquid phase	Solid phase	Air
ρ [kg m ⁻³]	6915.0	7800.0	1.0
c [J kg ⁻¹ K ⁻¹]	837.0	644.0	1008.2
λ [J s ⁻¹ m ⁻¹ K ⁻¹]	23.0	35.0	0.03
T_L [K]		1766.0	-
T_S [K]		1701.0	-
L [J kg ⁻¹]		270000.0	-
S_h [-]		0.02	-

The casting initially contains liquid alloy of temperature $T_0=1800$ K. Newton boundary conditions are defined on the external surfaces with $\alpha=20 \text{ J s}^{-1} \text{ m}^{-2} \text{ K}^{-1}$ and $T_\infty=300$ K on the top boundary while $\alpha=200 \text{ J s}^{-1} \text{ m}^{-2} \text{ K}^{-1}$ and $T_\infty=600$ K are assumed on the others. Neumann boundary condition is assumed on the plane of symmetry in the form of thermal insulation ($q_b=0 \text{ J s}^{-1} \text{ m}^{-2}$). Time step $\Delta t=0.25$ s is constant during the calculations. Evolving shrinkage cavities are treated as voids filled with air of properties shown in Table 1.

Figures 5-6 show temperature distribution in the casting as well as two shrinkage cavities after 125 and 350 s. Connected green spheres on the left pictures represent nodes filled with air. Because of the shape of the casting more than one macroscopic defect are observed. Main shrinkage cavity is observed in the upper part of the riser. The second void appears when the transport of the liquid through the narrow connection between the riser and the casting is stopped due to solid fraction growth. Temperature field in Figure 5 shows two separated volumes containing local thermal centres. These volumes are filled with liquid. Evolution of presented shrinkage cavities are caused by the solidification in these areas.

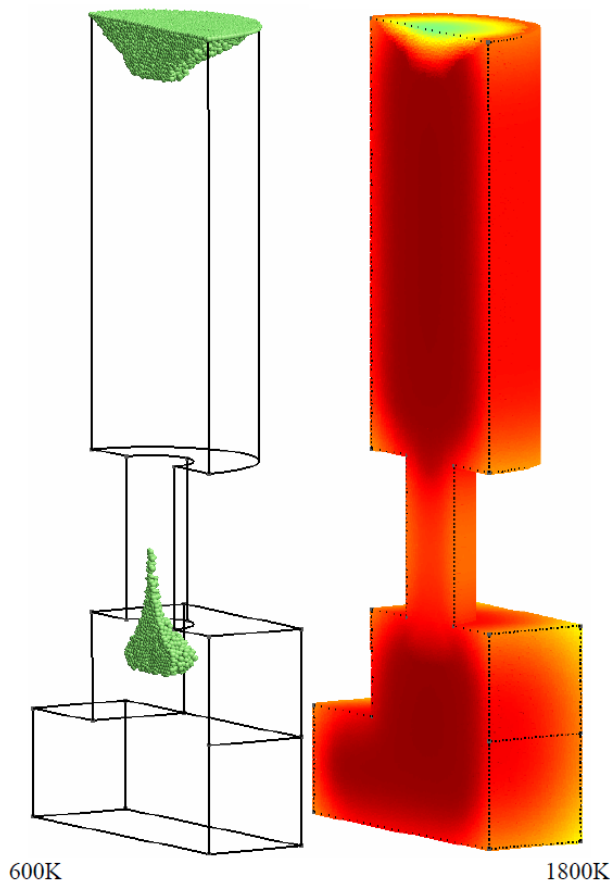


Fig. 5. Shrinkage cavities and the temperature field after 125 s

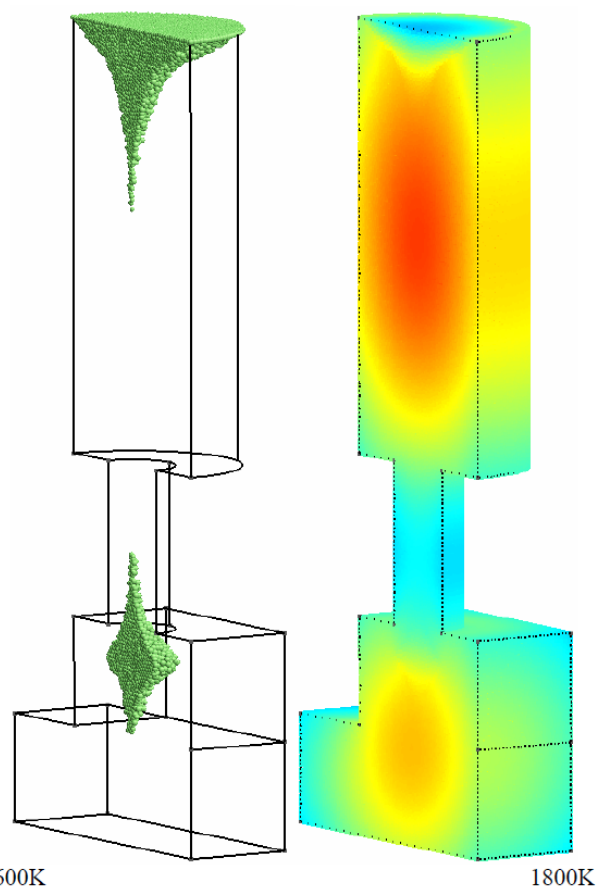


Fig. 6. Shrinkage cavities and the temperature field after 350 s

Figure 6 shows fully developed defects at the end of the solidification process ($f_s=1$ in the whole casting). Shrinkage cavity in the riser is acceptable but the second defect makes the casting unusable.

5. Conclusions

Mathematical and numerical descriptions of solidification process taking into account shrinkage cavity formation process have been discussed. Presented results of performed calculations show the effectiveness of used mathematical and numerical models as well as the computer implementation. Described approach is useful for modelling single macroscopic defect caused by the material contraction on solidification and also the multiple cavities associated with separated liquid areas. Original computer program developed on the base of FEM is robust and effective for complex three-dimensional geometries and boundary conditions. It's also free and more flexible than expensive commercial packages.

Further work is focused on the experimental validation of described model. It is very important to confirm that the simplifications of the algorithm of shrinkage cavities development process and material model are acceptable. Future work is also

focused on the introducing the geometry of the mould into the model and investigate its influence on the shrinkage cavities formation.

References

- [1] Pequet, Ch., Rappaz, M. & Gremaud, M. (2002). Modeling of microporosity, macroporosity, and pipe-shrinkage formation during the solidification of alloys using a mushy-zone refinement method: Applications to aluminum alloys. *Metallurgical and Materials Transactions A*. 33(7), 2095-2106.
- [2] Hajkowski, J., Roquet, P., Khamashta, M., Codina, E. & Ignaszak, Z. (2017). Validation tests of prediction modules of shrinkage defects in cast iron sample. *Archives of Foundry Engineering*. 17(1), 57-66. DOI: 10.1515/afe-2017-0011.
- [3] Campbell, J. (2003). *Castings*, (2nd ed.). Oxford: Butterworth-Heinemann.
- [4] Flemings, M.C. (1974). *The solidification processing*. New York: Mc Graw-Hill.
- [5] Jabur, A.S. & Kushnaw, F.M. (2017). Casting simulation and prediction of shrinkage cavities. *Journal of Applied & Computational Mathematics*. 6(4), 7. DOI: 10.4172/2168-9679.1000371.
- [6] Kim, C.J. & Ro, S.T. (1993). Shrinkage formation during the solidification process in an open rectangular cavity. *Journal of Heat Transfer*. 115(4), 1078-1081. DOI: 10.1115/1.2911369.
- [7] Zhang, C., Bao, Y., Wang, M. & Zhang, L. (2016). Shrinkage porosity criterion and its application to a 5.5 ton steel ingot. *Archives of Foundry Engineering*. 16(2), 27-32. DOI: 10.1515/afe-2016-0021.
- [8] Wu, M., Ludwig, A. & Kharicha, A. (2017). A four phase model for the macrosegregation and shrinkage cavity during solidification of steel ingot. *Applied Mathematical Modelling*. 41, 102-120. DOI: dx.doi.org/10.1016/j.apm.2016.08.023.
- [9] Mochnicki, B., Suchy, J.S. (1993). *Modeling and simulation of solidification of castings*. Warsaw: PWN. (in Polish).
- [10] Skrzypczak, T., Węgrzyn-Skrzypczak, E. & Sowa, L. (2019). Numerical model of solidification process of Fe-C alloy taking into account the phenomenon of shrinkage cavity formation. *MATEC Web of Conferences*. 254, 7. DOI: <https://doi.org/10.1051/mateconf/201925402009>
- [11] Geuzaine, C., & Remacle, J.-F. (2009). Gmsh: a three-dimensional finite element mesh generator with built-in pre- and post-processing facilities. *International Journal for Numerical Methods in Engineering*. 79(11), 1309-1331.